Dalton Transactions

ROYAL SOCIETY OF CHEMISTRY

PAPER

View Article Online
View Journal

Cite this: DOI: 10.1039/d1dt00214g

Multifunctional Pt(IV) prodrug candidates featuring the carboplatin core and deferoxamine†‡

Sophia Harringer, [a] Michaela Hejl,[a] Éva A. Enyedy, [b] Michael A. Jakupec, [a,c] Mathea S. Galanski,[a] Bernhard K. Keppler,[a,c] Paul J. Dyson [d] and Hristo P. Varbanov *[a,e]

Received 20th January 2021,
Accepted 2nd May 2021

DOI: 10.1039/d1dt00214g

rsc.li/dalton

The synergistic combination of the anticancer drug carboplatin and the iron chelator deferoxamine (DFO) served as a foundation for the development of novel multifunctional prodrugs. Hence, five platinum(IV) complexes, featuring the equatorial coordination sphere of carboplatin, and one or two DFO units incorporated at axial positions, were synthesized and characterized using ESI-HRMS, multinuclear (^{1}H, ^{13}C, ^{15}N, ^{195}Pt) NMR spectroscopy and elemental analysis. Analytical studies demonstrated that the chelating properties of the DFO moiety were not compromised after coupling to the platinum(IV) core. The cytotoxic activity of the compounds was evaluated in monolayer (2D) and spheroid (3D) cancer cell models, derived from ovarian teratocarcinoma (CH1/PA-1), colon carcinoma (SW480) and non-small cell lung cancer (A549). The platinum(IV)–DFO prodrugs demonstrated moderate *in vitro* cytotoxicity (a consequence of their slow activation kinetics) but with less pronounced differences between intrinsically chemoresistant and chemosensitive cell lines as well as between 2D and 3D models than the clinically used platinum(II) drug carboplatin.

Introduction

The pioneering work of Rosenberg led to platinum(II) complexes becoming first-line agents in antineoplastic therapy based on his discovery of the antiproliferative effects of cisplatin in the 1960s.[1] Subsequent research entailed the approval of cisplatin, carboplatin, and oxaliplatin (Fig. 1, a–c) for worldwide clinical use.[2–4]

Despite tremendous improvements, platinum-based drugs remain affected by severe dose limitations due to an array of side effects, or rendered ineffective by various resistance mechanisms.[3–5] Several strategies have been explored to address such drawbacks where the prodrug concept is one of the most promising approaches, with 15% of all newly approved drugs in 2001 and 2002 being prodrugs.[6] In this context, platinum(IV) complexes may be valuable alternatives to existing platinum(II)-based chemotherapy. One major advantage is that platinum(IV) complexes are characterized by enhanced kinetic inertness compared to their platinum(II) congeners, thus displaying a significantly lower ligand–exchange rate. This is of central importance for decreasing systemic toxicity and may enable oral administration and absorption *via* the gastrointestinal tract.[7–9] The two extra coordination sites introduced within the octahedral geometry of the platinum(IV) metal center allow numerous possibilities for chemical derivatization, modulation of physicochemical properties of interest (*e.g.* reduction rate and lipophilicity), as well as molecular targeting.[10–12] Furthermore, an altered mode of action is achieved, requiring activation by reduction (primarily in tumor tissue) to the respective platinum(II) congeners with release of two ligands, usually the axial ones.[10,13,14] So far, several platinum(IV) drug candidates (*e.g.* tetraplatin, iproplatin, satraplatin) have been evaluated in clinical trials, yet none have been approved for clinical use (Fig. 1, d–f).[15–17]

While the platinum(IV) candidates mentioned above release two biologically inactive groups upon reduction, another approach for ameliorating the pharmacological properties of the complex is to introduce bioactive ligands at the axial positions.[11,18] These so-called dual-threat (or dual-action, multifunctional) platinum(IV) agents usually consist of a classic

[a]*Institute of Inorganic Chemistry, University of Vienna, Waehringer Str. 42, 1090 Vienna, Austria. E-mail: hristo.varbanov@univie.ac.at*
[b]*Department of Inorganic and Analytical Chemistry, Interdisciplinary Excellence Centre, and MTA-SZTE Lendület Functional Metal Complexes Research Group, University of Szeged, Dóm tér 7, H-6720 Szeged, Hungary*
[c]*Research Cluster "Translational Cancer Therapy Research" University of Vienna, Waehringer Str. 42, 1090 Vienna, Austria*
[d]*Institut des Sciences et Ingénierie Chimiques, Ecole Polytechnique Fédérale de Lausanne (EPFL), CH-1015 Lausanne, Switzerland*
[e]*Institute of Chemistry – Inorganic Chemistry, University of Graz, Schubertstraße 1/III, 8010 Graz, Austria. E-mail: hristo.varbanov@uni-graz.at*

† Dedicated to Prof. Wolfgang Kaim on the occasion of his 70th birthday.

‡ Electronic supplementary information (ESI) available. See DOI: 10.1039/d1dt00214g

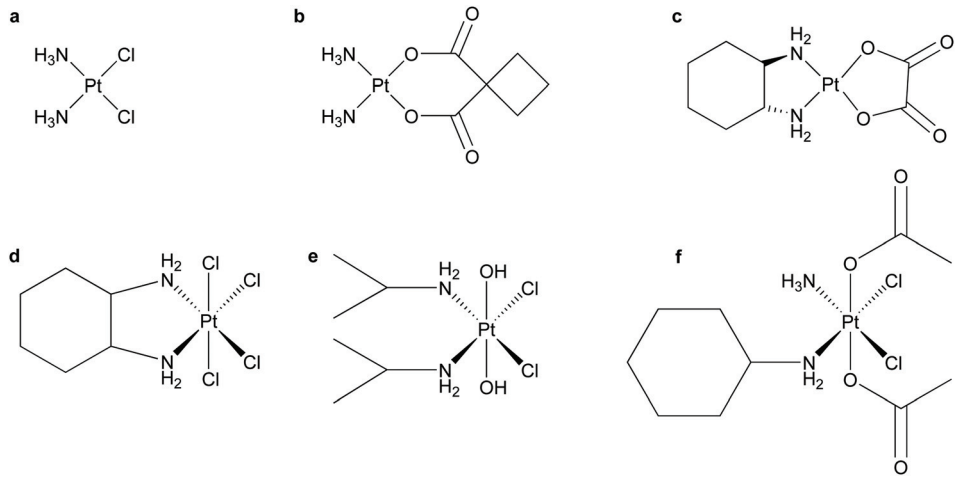

Fig. 1 Structures of the three platinum(II) drugs that are approved for clinical use worldwide: cisplatin (a), carboplatin (b), and oxaliplatin (c). Structures of three platinum(IV) complexes that underwent clinical trials: tetraplatin (d), iproplatin (e), and satraplatin (f).

platinum(II) anticancer drug unit and one or two biologically active axial ligands with a non–DNA target to overcome cross–resistance with the released platinum(II) chemotherapeutic.[8,14] Such platinum(IV) prodrugs resemble combination chemotherapy within a single molecule and a single pharmacokinetic profile, and they could provide new treatment options for chemoresistant cancers.[19,20] Mitaplatin and ethacraplatin (Fig. 2, g and h) are amongst the first examples of bifunctional platinum(IV) agents. Mitaplatin, the fusion product of cisplatin and the orphan drug dichloroacetate (DCA), was developed in order to selectively kill cancer cells *via* exploitation of their metabolic pathways.[21] Ethacraplatin was designed as a prodrug for cisplatin and ethacrynic acid, a potent inhibitor of glutathione-S-transferase (GST), in an attempt to overcome GST-related cisplatin resistance.[22,23] Other prominent examples comprise platinum(IV) derivatives of cisplatin or oxaliplatin, bearing cyclooxygenase (COX) inhibitors (*e.g.*, aspirin, ibuprofen, indomethacin),[24,25] histone deacetylase inhibitors (*e.g.*, valproate or phenylbutyrate)[26,27] or chalcone derivatives[28] at axial positions. Recently, platinum(IV) complexes featuring two different non-innocent axial ligands have also been reported, where the second axial ligand introduces another

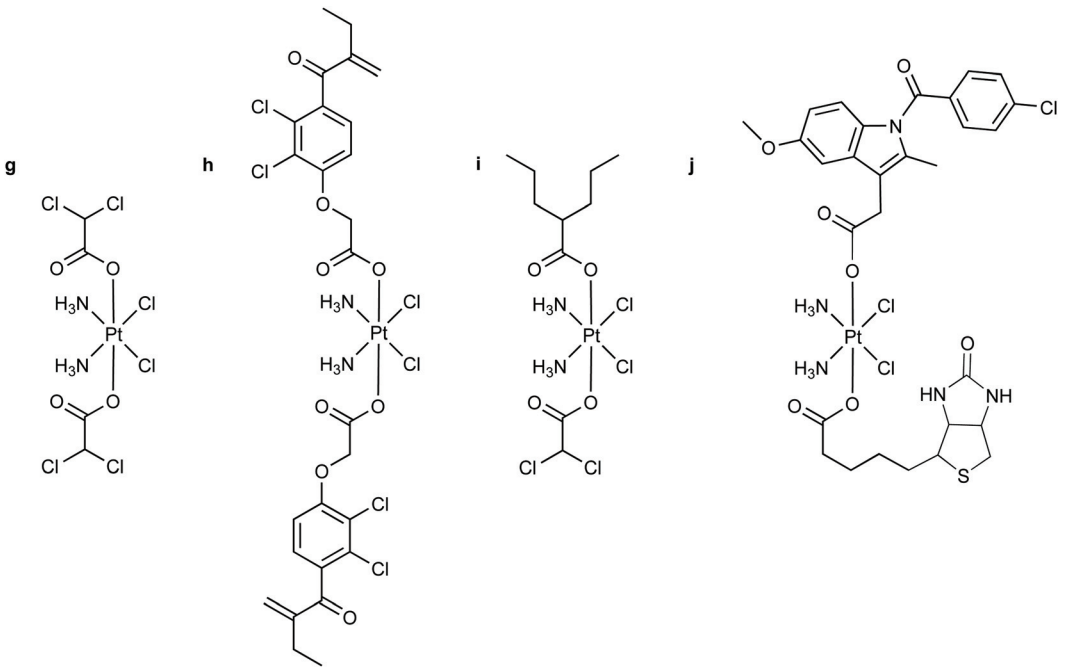

Fig. 2 Examples for multifunctional platinum(IV) prodrug candidates: mitaplatin (g), ethacraplatin (h), a triple-action agent featuring DCA and valproate (HDACi) (i), and a targeted dual-action agent featuring indomethacin (COX inhibitor) and biotin (cancer targeting group) (j).

bioactivity (triple-action compounds)[29] or targeted properties (Fig. 2, i and j).[30,31] Finally, a "quadruple-action" dinuclear platinum(IV) complex, which can release four different bioactive moieties (*i.e.*, cisplatin, DCA, phenylbenzoate and Pt56MeSS) upon intracellular reduction was reported.[32]

In this context, it is worth mentioning the bioactive compound deferoxamine (desferrioxamine B, DFO, see Fig. 3). DFO was introduced into clinical usage in the 1960s and is still being used in treatments of iron overload disorders.[33,34] DFO is also utilized as a chelating agent in the development of ^{89}Zr-labeled molecular probes for PET imaging,[35] while its lipophilic derivatives have been investigated as potential therapeutic agents for Parkinson's disease.[36] Besides its metal chelating properties utilized to remove excess iron or aluminum ions, DFO also exhibits anticancer activity, which was demonstrated in several studies, including a phase I clinical trial in patients with hepatocellular carcinoma.[37–39] The mechanism of its antiproliferative activity is based on several regulatory proteins, which are responsible for the expression of cell cycle control molecules (*e.g.*, p53 and Cdk2), and dependent on iron concentration.[40] Finally, a recent study revealed strong synergistic interactions between DFO and carboplatin in A549 (NSCL) cells and highlighted the potential utility of this combination as a basis for the development of new platinum-based treatments, including multifunctional prodrugs.[41]

Accordingly, we aimed to develop a series of platinum(IV) complexes, featuring the equatorial coordination sphere of carboplatin, and DFO coupled to one or both of the axial ligands through its pendant terminal amino group. Succinic acid esters were chosen as linkers as they should provide an optimal solubility/lipophilicity balance, as well as sufficient solution stability under physiologically relevant conditions.[42] While many cisplatin-based dual-threat prodrugs have been studied, at this time carboplatin-based agents are rare.[43] Herein, we report the synthesis and characterization of five new multifunctional platinum(IV) complexes designed as prodrugs for carboplatin and DFO. The cytotoxic activity of the new compounds was evaluated in monolayer (2D) and spheroid (3D) cancer cell cultures. Their Fe(III) binding properties and the effect of Fe(III) loading on cytotoxicity were also investigated.

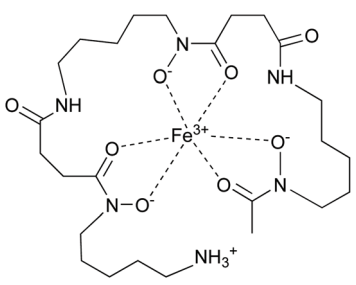

Fig. 3 Structure of DFO chelating an Fe(III) ion; the terminal amino group is protonated at physiological pH.

Results and discussion

Synthesis

The dual-action Pt(IV) complexes in this work are based on a carboplatin scaffold and were synthesized according to the routes shown in Fig. 4. In the first step carboplatin was oxidized with 30% (w/w) H_2O_2 in water to afford dihydroxidoplatinum(IV) complex **1** in excellent yield. Subsequent carboxylation of **1** with excess succinic anhydride in dry DMF at 50 °C gave bis(succinato) precursor **5** with yields over 85%.[44] Performing the reaction in dry DMSO at room temperature and with only one equivalent of succinic anhydride allowed the synthesis of the monosuccinato precursor **2** in 70% yield. Precursors **3** and **4** were obtained after treatment of **2** with an excess of either acetic or propionic anhydride in dry DMF solutions at 45 °C with yields of 69% and 54%, respectively. Notably, it was observed, that this route for synthesis of **3**, comprising an additional reaction step, was superior to direct unsymmetrical oxidation in acetic acid, followed by treatment with succinic anhydride, which led to mixtures of the desired product and the bis(acetato) analogue. Indeed, the herein presented synthesis of non-symmetric platinum(IV) complexes represents a straightforward procedure with a simple reaction work-up. Additionally, the spectrum of precursors featuring free carboxylic groups is broadened by this work, as isolation of similar products was found to be difficult in some cases.[42]

Finally, the target platinum(IV)–DFO conjugates (**A–E**) were synthesized from precursors **2–5** *via* activation of their free carboxylic group(s) with CDI in dry DMF[44,45] and subsequent reaction with DFO. Final products were obtained after purification by preparative reversed phase high-performance liquid chromatography (RP-HPLC) and lyophilization, in yields of 10–20%. In the case of the bis(succinato) precursor **5**, a mixture of mono- and bis-DFO conjugates (**D** and **E**, respectively), was obtained. The latter could be separated by preparative RP-HPLC, affording **D** and **E** as pure products.

Characterization

^{1}H, ^{13}C, ^{15}N, and ^{195}Pt one- and two-dimensional NMR spectroscopic investigations were carried out to characterize the complexes. Identity and purity of target compounds **A–E** were additionally verified by electrospray ionization high-resolution mass spectra (ESI-HRMS), ultra-high performance liquid chromatography (UHPLC) and elemental analysis. Complexes **B–E** could be obtained in >95% purity as confirmed by elemental analysis and analytical RP-UHPLC (both isocratic and gradient conditions). In the case of complex **A**, HPLC purity >85% could not be reached after multiple cycles of preparative RP-HPLC (see Fig. S1‡).

^{195}Pt NMR spectra of the new complexes afforded peaks between 3300–3600 ppm (Table 1), in accordance with other platinum(IV) derivatives of carboplatin featuring axial carboxylates.[44,46] Most significant changes in the ^{195}Pt resonances were found for carboxylation of platinum coordinated hydroxido ligands which was accompanied by shifts to lower field of around 170 (compare **2** to **3**) or 190 ppm (compare **A**

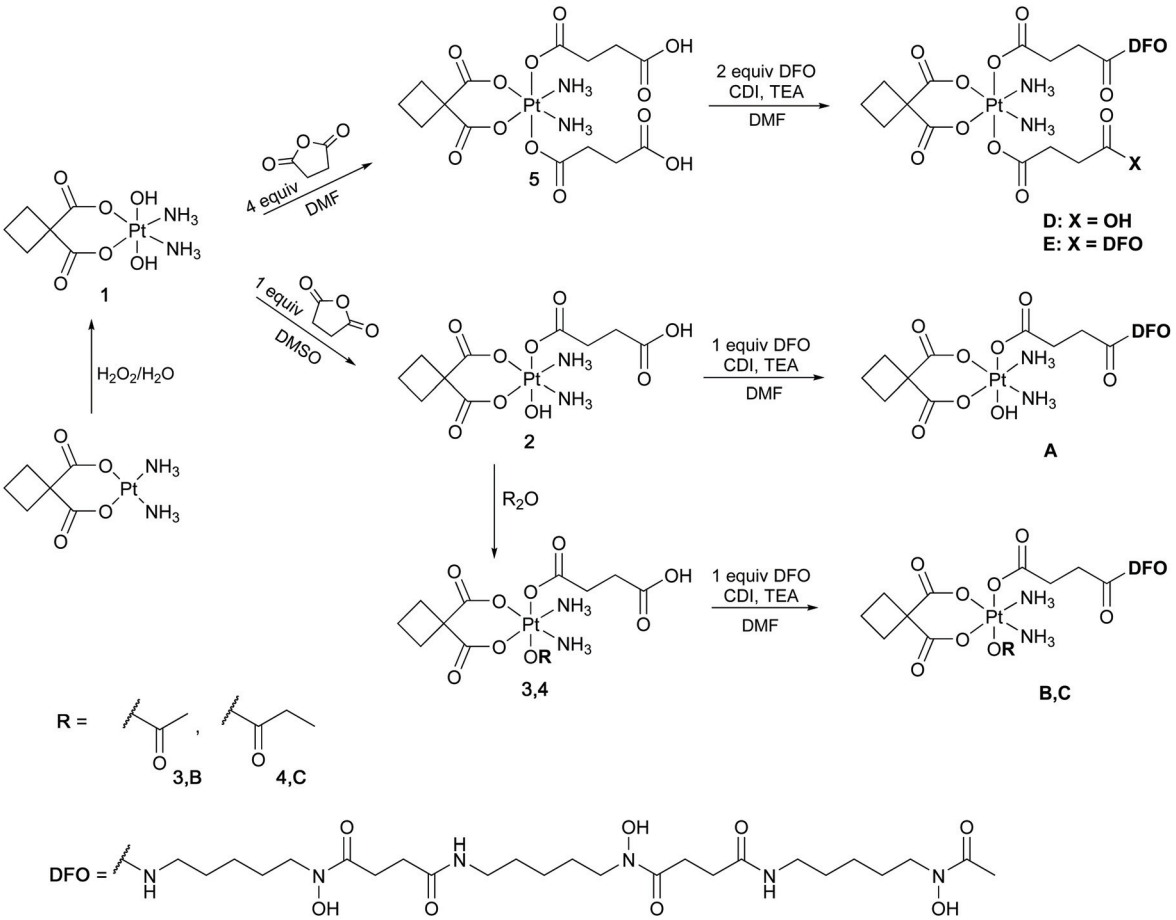

Fig. 4 Synthetic routes used to prepare the Pt(IV)–DFO conjugates with a carboplatin core; CDI = 1,1′-carbonyldiimidazole, TEA = triethylamine.

Table 1 ^{195}Pt and ^{15}N NMR chemical shifts of precursors **2–5**, and complexes **A–E** in d_6-DMSO, or d_7-DMF (**3**, **5**) in ppm

Complex	^{195}Pt	^{15}NH	^{15}NH$_3$
2	3385	—	−51.5
3	3560	—	−54.4
4	3572	—	−51.6
5	3565	—	−53.8
A	3382	94.9	−51.6
B	3573	95.0	−53.0
C	3574	95.3	−51.8
D	3580	94.7	−52.7
E	3576	94.8	−52.7

with **B** and **C**), respectively. Changes at the peripheral sites, however, had only a marginal influence on the frequency of the peaks in the ^{195}Pt NMR spectra.

Identity of platinum(IV)–DFO conjugates (**A–E**) was unequivocally confirmed by ESI-HRMS measurements. MS signals corresponding to single and doubly charged molecular ions of the complexes were observed in both positive and negative ion mode spectra. In the case of bisconjugate **E**, triple-charged species were also detected (*i.e.*, $[M + 3Na^+]^{3+}$ and $[M - 3H^+]^{3-}$).

Pharmacologically relevant physicochemical properties

Platinum(IV)–DFO conjugates are well soluble in DMSO and sparingly soluble in water (1–2 mg mL^{-1}), with bisconjugate **E** being the least water soluble compound (<0.5 mg mL^{-1}). Stability in water and buffered solutions (pH 7.4) was monitored by ^{1}H NMR spectroscopy and RP-UHPLC. No signs of decomposition were observed over 24 h of incubation at room temperature. The compounds are also stable in the presence of simple biological reductants (*i.e.*, ascorbate), in line with the kinetic stability to reduction reported for other tertracarboxylatoplatinum(IV) complexes[46,47] (see Fig. S2‡). RP-HPLC-derived chromatographic lipophilicity parameters $\log k_w$ and φ_0 were determined for the new multifunctional compounds in order to estimate their ability to cross cell membranes *via* passive diffusion. Chromatographic lipophilicity parameters are easy to assess and known to have good correlation with the partition coefficient $\log P_{o/w}$.[48,49] The platinum(IV)–DFO conjugates displayed relatively moderate lipophilicity ($\log k_w$ = 3.5–5, φ_0 = 48–55), and are significantly more lipophilic than carboplatin ($\log k_w$ = −0.02). Among the studied platinum(IV) complexes, **C** and **E** are the most lipophilic (Table S1‡). In summary, new platinum(VI)–DFO complexes exhibit favorable physicochemical properties, enabling their potential use as prodrugs.

Interactions with Fe^{3+}, Zn^{2+} and Zr^{4+} ions

Free DFO has a very high affinity and specificity for Fe^{3+} ($\log\beta$ (Fe(III)LH) = 41.01 and $\log\beta$ (Fe(III)L) = 30.4, where L is the completely deprotonated form of the ligand).[50] The tris-chelated mono-ligand FeLH complex predominates at physiological pH, in which the octahedral coordination sphere of the metal ion is saturated by the three binding hydroxamate groups and the terminal amino moiety is protonated (see Fig. 3).[51,52] The high Fe(III) binding affinity of DFO enables it to remove iron from ferritin and hemosiderin, but not from haemoglobin and only to small extent from transferrin. Furthermore, its affinity to other physiologically relevant metal ions is much lower[53] (*e.g.*, $\log\beta$ (Fe(II)L) = 10,[54] $\log\beta$ (Cu(II)L) = 13.73,[55] $\log\beta$ (Zn(II)L) = 10.36,[55] $\log\beta$ (Ca(II)L) = 3.03.[50]). In order to test if the chelating properties of the DFO moiety remain intact after coupling to the Pt(IV) core, platinum(IV)–DFO conjugates were co-incubated with the endogenous Fe(III) and Zn(II) ions, and complexation reactions were studied by RP-UHPLC and ESI-HRMS. In addition, the binding affinity towards $ZrCl_4$ was also checked to monitor the potential application of these platinum(IV) complexes as ^{89}Zr(IV) carriers. Measurements confirm the formation of Fe(III) and Zr(IV) adducts (see chromatograms and MS spectra in Fig. S3–S5 and S8–S10‡). In contrast, co-incubation with $ZnCl_2$ resulted in no changes in the chromatogram over 24 h under the same experimental conditions (Fig. S6 and S7‡), in agreement with the much lower affinity of DFO towards Zn^{2+} ions. Zn(II) adducts were observed in the MS spectra, however with low relative intensities and only in positive ion mode.

For a deeper insight into the Fe(III) binding ability of platinum(IV)–DFO conjugates, the conditional stability constants ($\log\beta'_{7.4}$ (Fe(III)L)) for the Fe(III) adducts of **B** and **D** were determined at pH 7.4 using UV-visible spectrophotometry. Bis-conjugated complex **E** was not included in these studies, due to its limited aqueous solubility. The Fe(III)–deferoxamine (1 : 1) system was also assayed for comparison. Additionally, the pH dependence of the UV-visible spectra of the Fe(III)–complex **B** or **D** or DFO (1 : 1) systems was monitored. The spectra recorded for the platinum(IV) complexes remained unaltered in the pH range from 2.3 to 11.5; however, changes were observed at pH < 2 (see Fig. S11a‡ for the Fe(III) complex of **B**). Similarly to the Fe(III) complex of DFO,[50] the λ_{max} shifted to higher values with decreasing pH (Fig. S11b‡) due to the rearrangement from tris-hydroxamato to bis-hydroxamato coordination mode. In the basic pH range (pH > 11) the spectra of the Fe(III) complexes of **B** and **D** did not change. The DFO complex behaves differently, with a minimal absorbance decrease attributed to the deprotonation of the non-coordinating terminal amino group (pK_a = 10.6).[50] These findings indicate the formation of high stability Fe(III) complexes with **B** and **D** over a wide pH range including the physiological pH. Deferiprone, a bidentate Fe(III) chelator, was added stepwise to the equimolar solution of the platinum(IV) complex and Fe(III) at pH 7.4, and UV-visible spectra were recorded (see Fig. 5a for complex **B**). Upon addition of the competitor ligand deferiprone, the spectra revealed significant change, *i.e.* both λ_{max} and absorbance values increased due to the formation of the tris-ligand Fe(III)-deferiprone complex. The spectra were deconvoluted in order to compute the conditional stability constants for the Fe(III) complexes of **B** and **D** (and for DFO for comparison) using the overall stability constants of the Fe(III) complexes of deferiprone ($\log\beta$ values for FeL = 14.56, FeL_2 = 26.75, FeL_3 = 36.44)[56] and its pK_a values (3.68; 9.77).[56] The fit between the measured and computed absorbance values are shown in Fig. 5b for complex **B**, and concentration-distribution curves representing the ligand displacement process are presented in Fig. S12.‡ Log $\beta'_{7.4}$ (Fe(III)L) as 24.34 ± 0.01, 24.53 ± 0.02 and 25.45 ± 0.05 were estimated for the Fe(III) complexes of compounds **B**, **D** and DFO, respectively. It should be noted that a $\log\beta$ (Fe(III)LH) = 40.90 overall stability constant can be calculated for DFO from this conditional constant that corresponds well with the reported value (41.01).[50] The obtained conditional stability constants represent the similar, but somewhat lower, Fe(III) binding ability of the tested Pt(IV) complexes in comparison to DFO.

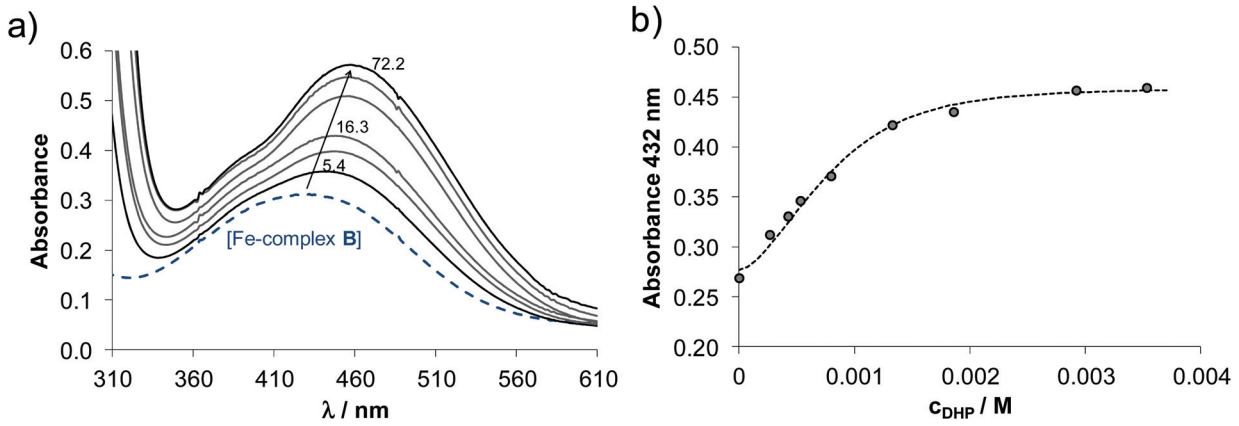

Fig. 5 (a) UV-Visible spectra of the Fe(III)–complex **B** (1 : 1) upon addition of deferiprone at pH 7.4 (numbers indicate the complex-to-deferiprone ratios). (b) Absorbance values at 432 nm at the various deferiprone concentrations (●) plotted together with the fitted values (dashed line). ($c_{Fe(III)}$ = c_B = 50 μM, $c_{deferiprone}$ = 0–3.61 mM, T = 25 °C, ionic strength = 0.20 M KCl, path length = 1 cm).

The redox potentials of the Fe(III) complexes of compounds **B** and **D** were determined by cyclic voltammetry at pH 7.4 in aqueous solution (Fig. S13‡), with values of formal potential E'^{o} = −455 mV and −459 mV *vs.* normal hydrogen electrode (NHE) obtained, respectively, which are slightly higher than that of the DFO complex (−480 mV *vs.* NHE).[54] These data also confirm the small difference in the Fe(III) binding pattern and strength of the platinum(IV) complexes and DFO. No $Pt^{IV} \rightarrow Pt^{II}$ reduction was observed under these conditions (potential window between −0.8 and −0.2 V).

Cytotoxicity in 2D and 3D cell culture models

The antiproliferative activity of platinum(IV)–DFO conjugates **A–E** was determined using the colorimetric MTT assay in three human cancer cell lines, CH1/PA-1 (ovarian teratocarcinoma), SW480 (colon carcinoma), and A549 (non-small cell lung cancer). Carboplatin and DFO were also examined for comparison. The obtained IC_{50} values are given in Table 2 and concentration-effect curves of the platinum(IV) complexes are shown in Fig. S14.‡

As expected, the platinum compounds displayed higher cytotoxicity in cis/carboplatin-sensitive CH1/PA-1 cells than in the intrinsically chemoresistant SW480 and A549 cells. However, these differences were much more pronounced for carboplatin (~50-fold), than for the new platinum(IV) complexes (~3.5- to 14-fold). Overall, all of the new Pt(IV)–DFO conjugates demonstrated a fairly comparable potency in CH1/PA-1 cells. Somewhat larger differences were observed in SW480 and A549 cells where compounds **D** and **E** showed ~2–7 times lower IC_{50} values (compared to **A–C**). It is also worth mentioning that DFO showed comparable (in CH1/PA-1 cells) and up to 10 times higher (in chemoresistant SW480 and A549 cells) activity than the clinically used platinum(II) drug carboplatin. Nevertheless, the presence of a second DFO moiety in platinum(IV) complex **E** did not result in an increase of activity compared to analog **D**.

To explore the effect of Fe(III) loading on the cytotoxicity of new platinum(IV)–DFO conjugates, complex **B** was co-incubated with $FeCl_3$ (1 : 1) and its activity towards cancer cell lines was examined. MTT experiments revealed that $FeCl_3$ has no significant influence on the cytotoxicity of complex **B** in SW480 and A549 cells (see Fig. S15‡).

In order to gather further insights into the pharmacological behavior of the new platinum(IV) complexes, the cytotoxicity of selected compounds was examined in CH1/PA-1 multicellular tumor spheroids (see Table 3 and Fig. S16‡). 3D cancer cell models, such as spheroids, resemble solid tumors more closely than the respective 2D monolayer systems,[57] which is commonly associated with decreased cytotoxicity of tested substances.[58] Accordingly, 50% inhibition of cell viability was reached at higher concentrations in spheroids compared to conventional 2D cultures for all examined compounds. More pronounced increases of the IC_{50} values were observed for DFO and carboplatin (8 and 12 times, respectively), whereas in the case of platinum(IV) complexes **B** and **D**, differences were less marked (~2.5 and ~4.5 times, respectively). This suggests a fairly high capacity of penetrating into the spheroids and/or a fairly low dependency of their effects on cell cycle activity.

Finally, combination effects between carboplatin and DFO in the tested cell lines were evaluated with the combination index (CI) method of Chou and Talalay.[59,60] Synergistic interactions between the drugs were confirmed in A549 and CH1/PA-1 monolayer cultures, as well as CH1/PA-1 spheroids, but not in SW480 monolayers, where additive to antagonistic effects were observed (see Table S2‡ and Fig. 6). These results confirm our previous findings revealing synergistic interactions between carboplatin and DFO in cells cultures from lung origin (A549, MRC-5), but not from human colorectal carcinoma (HCT116).[41]

Platinum(IV)–DFO conjugates showed generally lower *in vitro* cytotoxicity than carboplatin (except for complex **D** in A549 cells), presumably due to their slow rate of activation. These results are in line with previous reports on tetracarboxylatoplatinum(IV) complexes, exhibiting lower cytotoxicity than their Pt(II) counterparts, regardless of the lipophilicity of their axial ligands.[44,46] Moreover, carboplatin and Pt(IV) complexes bearing a carboplatin core have shown much lower accumulation in SW480 cells than cisplatin and Pt(IV) analogues with a cisplatin-like core.[47] In this context, it could be assumed that new Pt(IV)–DFO conjugates behave similarly to other carboplatin prodrugs. Further experiments, especially the use of relevant *in vivo* models, are required to fully assess the chemother-

Table 2 Cytotoxicity of investigated platinum(IV)–DFO complexes in comparison to carboplatin and DFO in three human cancer cell lines (MTT assay, 96 h exposure)

	IC_{50} [μM]		
Compound	CH1/PA-1	SW480	A549
A[a]	14 ± 4	168 ± 9	174 ± 27
B	18 ± 1	215 ± 46	254 ± 24
C	23 ± 4	255 ± 19	297 ± 13
D	12 ± 3	78 ± 6	42 ± 6
E	13 ± 2	89 ± 22	72 ± 15
Carboplatin	0.79 ± 0.11	42 ± 10	38 ± 3
DFO	1.0 ± 0.1	6.6 ± 1.3	4.0 ± 0.8

[a] RP-HPLC determined purity of complex **A** (~85%) does not meet the purity criteria (>95%) for biological tests and thus the obtained IC_{50} values must be taken with caution.

Table 3 IC_{50} values of selected compounds in CH1/PA-1 multicellular tumor spheroids (based on resazurin staining of undissociated spheroids at the end of 96 h exposure to test compounds) and ratios of IC_{50} values in spheroid (3D) and monolayer (2D) cultures

	IC_{50} [μM]	
Compound	CH1/PA-1	3D/2D
B	46 ± 2	2.6
D	55 ± 18	4.6
Carboplatin	9.9 ± 2.8	12.5
DFO	8.4 ± 0.9	8.4

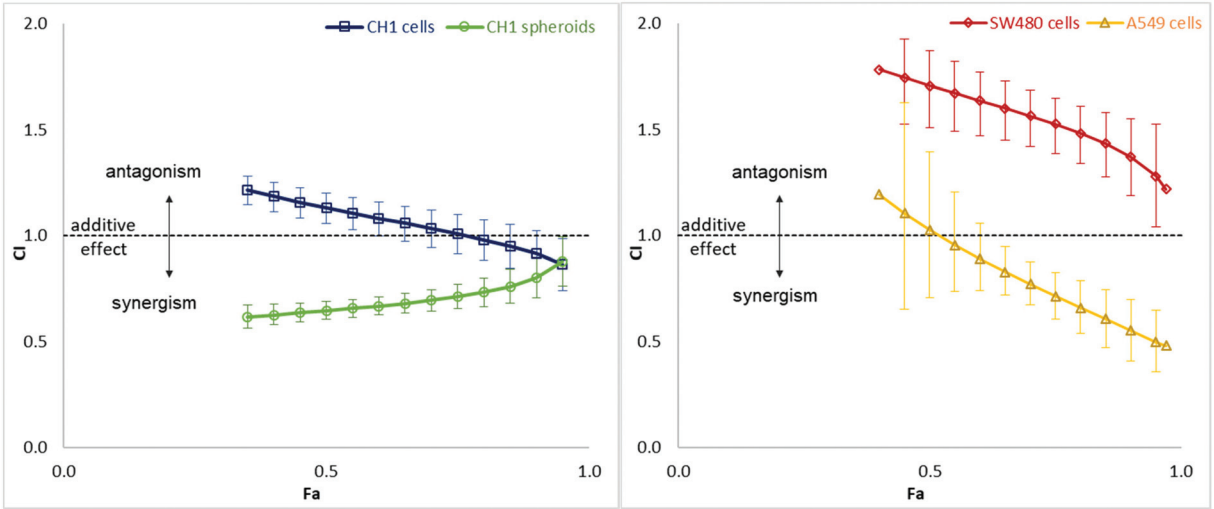

Fig. 6 Combination effects between carboplatin and DFO (molar ratio, 1 : 1). Fa-CI plot in CH1 monolayer cultures and spheroids (left), and A549 and SW480 monolayer cultures (right). The fraction of effect (Fa between 0 and 1) corresponds to the cell viability inhibition effect. Error bars represent 95% confidence intervals of the CI (combination index) variability at the presented effect levels, as determined by sequential deletion analysis.

apeutic potential of these multifunctional complexes; of particular interest are the mechanism and kinetics of activation *in vivo*, the synergistic interactions between the products released, as well as the ability to chelate free Fe(III) and the potential for targeted delivery.

Conclusion

A series of five multifunctional platinum(IV) agents with a carboplatin core and DFO tethered to one or both of the axial ligands were synthesized and studied in detail by various analytical techniques. New platinum(IV)–DFO complexes demonstrated favorable physicochemical properties (*e.g.*, lipophilicity and stability), enabling their potential use as prodrugs. The ability of DFO to chelate Fe(III) and Zr(IV) was not affected after conjugation to the platinum(IV) core. Thus, platinum(IV)–DFO conjugates could express multiple biological effects *in vivo* and may serve as theranostic agents after radiolabeling with ^{89}Zr. *In vitro* cytotoxicity experiments in 2D and 3D cancer cell cultures revealed moderate activity of the new complexes in line with other prodrugs of carboplatin. The most active compounds reached 50% inhibition of cell viability in chemoresistant cell models at similar concentrations with the clinically used platinum(II) drug carboplatin.

Experimental section

Materials and methods

All reagents and solvents were obtained from commercial suppliers and used without further purification. Reactions were carried out under light protection and with glass coated magnetic stirring bars. Water used for reactions was purified by reverse osmosis, followed by double distillation. Milli-Q water (18.2 MΩ cm, Merck Milli-Q Advantage, Darmstadt, Germany) was used for HPLC experiments. Preparative HPLC was carried out on a Xbridge BEH C18 OBD prep column (19 mm × 250 mm, 10 μm) at room temperature, a flow rate of 17 ml min^{-1} and under UV-Vis detection. Analytical UHPLC experiments were performed on an Ultimate 3000 Dionex system, equipped with Waters Acquity BEH C18 column (3.0 mm × 50 mm, 1.7 μm), at 25 °C, a flow rate of 0.6 ml min^{-1} and UV-Vis detection. Mobile phases consisted of water and acetonitrile or methanol (HPLC grade, with 0.1% formic acid) mixtures. NMR spectra were recorded on a Bruker Avance NEO 500 MHz NMR spectrometer at 500.32 (^{1}H), 125.81 (^{13}C), 50.70 (^{15}N) and 107.55 (^{195}Pt) MHz in D_2O, DMF-d_7 or DMSO-d_6 at 298 K. Chemical shifts were reported in parts per million (ppm). As internal standards for ^{1}H and ^{13}C spectra, solvent resonances were used (DMF-d_7, 2.93 ppm, DMSO-d_6, 2.50 ppm and D_2O, 4.79 ppm for ^{1}H; DMSO-d_6, 39.5 ppm and DMF-d_7, 34.8 ppm for ^{13}C). As external standards for ^{195}Pt and ^{15}N NMR spectra, $K_2[PtCl_4]$ and NH_4Cl were used, respectively. Electrospray ionization high-resolution mass spectra (ESI-HRMS) were obtained using a Bruker maXis ESI-QqTOF spectrometer. Measurements were conducted in both positive and negative ion mode using acetonitrile (MeCN)/methanol (MeOH) 1% H_2O as solvent. Elemental analyses (C, H, N) were carried out at the Microanalytical Laboratory at the Faculty of Chemistry of the University of Vienna with a PerkinElmer 2400 CHN Series II or a Eurovector EA3000 elemental analyser, and are within ±0.4% of the calculated values.

Synthesis and characterization

Carboplatin, its dihydroxidoplatinum(IV) analogue (**1**) and precursor **5** were prepared according to standard methods reported in literature.[44,61] Precursors **2–4** were obtained by fol-

lowing an improved procedure, which allowed an increase in product purity and overall yield.

(*OC*-6-44)-Diammine(3-carboxypropanato)(cyclobutane-1,1-dicarboxylato)hydroxidoplatinum(IV) (2). (*OC*-6-33)-Diammine(cyclobutane-1,1-dicarboxylato)dihydroxidoplatinum(IV) (**1**, 432 mg, 1.07 mmol, 1 equiv.) was suspended in dry DMSO (24 mL) under argon atmosphere. Succinic anhydride (107 mg, 1.07 mmol, 1 equiv.) was added and the reaction mixture was stirred for 24 h at RT. The obtained turbid solution was filtered and the filtrate was concentrated to dryness at 35 °C *in high vacuo*. The crude product was obtained as a white solid. Purification was carried out *via* resuspension in MeOH (15 mL) and stepwise precipitation with acetone and diethyl ether. The precipitates were filtered off, washed with cold Et_2O and dried *in vacuo*. **2** was obtained as a white powder (363 mg, 68%). ^{1}H NMR (500.32 MHz, DMSO-d_6): δ 11.97 (s, 1H, COO*H*), 6.11–5.65 (m, 6H, NH_3), 2.57–2.53 (m, 2H, H2/H3), 2.42 (dd, J = 10.9, 4.2 Hz, 2H, H4), 2.36 (dd, J = 10.6, 3.9 Hz, 2H, H5), 1.84–1.74 (m, 2H, H1) ppm. ^{13}C NMR (125.81 MHz, DMSO-d_6): δ 179.5 (C4′), 177.0 (C2′/C3′), 174.5 (C5′), 56.1 (C1′), 32.7 (C4), 31.4 (C2/C3), 30.4 (C5), 16.3 (C1) ppm. ^{15}N NMR (50.70 MHz, DMSO-d_6): δ −51.5 ppm. ^{195}Pt NMR (107.55 MHz, DMSO-d_6): δ 3385 ppm.

General procedure for synthesis of unsymmetrical Pt(IV) precursors (3–4)

Complex **2** and 4 equiv. of the corresponding anhydride were suspended in dry DMF and the reaction mixture was stirred for 4 h at 45 °C under argon atmosphere. The obtained solution was filtered from undissolved particles and the solvents were removed under reduced pressure at 35 °C. Purification of the crude product was done *via* resuspension in MeOH and precipitation with acetone. The final product was washed with cold acetone and Et_2O, and dried *in vacuo*. Complexes **3** and **4** were obtained as white powders.

(*OC*-6-44)-(Acetato)diammine(3-carboxypropanoato)(cyclobutane-1,1-dicarboxylato)platinum(IV) (3). Acetic anhydride (250 μL, 2.68 mmol) and **2** (300 mg, 0.60 mmol) in DMF (12 mL). Yield (228 mg, 69%). ^{1}H NMR (500.32 MHz, DMSO-d_6): δ 12.08 (s, 1H, COO*H*), 6.64–6.12 (m, 6H, NH_3), 2.57–2.54 (m, 4H, H2/H3), 2.53–2.50 (m, 2H, H4), 2.46–2.43 (m, 2H, H5), 1.91 (s, 3H, H6), 1.83–1.74 (m, 2H, H1) ppm. ^{13}C NMR (125.81 MHz, DMF-d_7): δ 179.6 (C4′), 178.1 (C6′), 176.8 (C2′/C3′), 173.9 (C5′), 56.2 (C1′), 32.1 (C4/C5), 31.5 (C2/C3), 21.7 (C6), 15.8 (C1) ppm. ^{15}N NMR (50.70 MHz, DMF-d_7): δ −54.4 ppm. ^{195}Pt NMR (107.55 MHz, DMF-d_7): δ 3560 ppm.

(*OC*-6-44)-Diammine(3-carboxypropanoato)(cyclobutane-1,1-dicarboxylato)(propionato)platinum(IV) (4). Propionic anhydride (613 μL, 4.78 mmol) and **2** (604 mg, 1.20 mmol) in DMF (12 mL). Yield (360 mg, 54%). ^{1}H NMR (500.32 MHz, DMSO-d_6): δ 12.09 (s, 1H, COO*H*), 6.34–6.11 (m, 6H, NH_3), 2.56–2.53 (m, 4H, H2/H3/H4), 2.37–2.35 (m, 2H, H5), 2.27–2.24 (m, 2H, H6), 1.82–75 (m, 2H, H1), 0.93 (t, J = 7.5 Hz, 3H, H7) ppm. ^{13}C NMR (125.81 MHz, DMSO-d_6): δ 180.6 (C4′), 179.1 (C6′), 176.8 (C2′/C3′), 174.2 (C5′), 56.0 (C1′), 31.9 (C4/C5), 30.6 (C6), 28.8 (C2/C3), 16.1 (C1), 9.6 (C7) ppm. ^{15}N NMR (50.70 MHz, DMSO-d_6): δ −51.6 ppm. ^{195}Pt NMR (107.55 MHz, DMSO-d_6): δ 3572 ppm.

General procedure for synthesis of Pt(IV)–DFO conjugates (A–E)

CDI (1.1 equiv. in the case of **A–C** and 2.2 equiv. in the case of **D**/**E**) and 1 equiv. of the respective Pt(IV) precursor were dissolved in dry DMF and heated to 60 °C for 10 min. After cooling to RT, formed CO_2 was removed by flushing the solution with argon for 10 min. Afterwards, a solution containing 1.0 equiv. of DFO·mes and 2.0 equiv. of TEA (double amounts for **D**/**E**) in dry DMSO was added and the resulting mixture was stirred for 48 h at RT. DMF and DMSO were removed under reduced pressure at 35 °C. The crude product was obtained after resuspending in MeOH and stepwise precipitation with MeOH and MeCN. Purification was performed *via* preparative RP-HPLC. Collected pure fractions were combined and lyophilized to give the final product as a white powder.

(*OC*-6-44)-Diammine(cyclobutane-1,1-dicarboxylato)(hydroxido)(3,14,25-trihydroxy-2,10,13,21,24,32-hexaoxo-3,9,14,20,25,31-hexaazapentatriacontan-35-oato)platinum(IV) (A). **2** (505 mg, 1.00 mmol) and CDI (178 mg, 1.10 mmol) in DMF (19 mL). DFO·Mes (657 mg, 1.00 mmol) and TEA (278 μL, 2.00 mmol) in DMSO (6 mL). Preparative RP-HPLC gradient conditions (H_2O/MeOH): 0–6 min (10% MeOH), 6–21.0 min (10–25% MeOH), 21.1–26.0 min (95% MeOH), 26.1–28.1 min (10% MeOH); the product eluted at 17.8 min. Yield (64 mg, 8%). ^{1}H NMR (500.32 MHz, DMSO-d_6): δ 9.70 (s, 3H, H12/H21/H30), 7.84–7.76 (m, 3H, H6/H15/H24), 6.10–5.68 (m, 6H, NH_3), 3.47–3.42 (m, 6H, H11/H20/H29), 3.03–2.95 (m, 6H, H7/H16/H25), 2.59–2.51 (m, 4H, H13/H22), 2.50 (under DMSO, 4H, H2/H3), 2.48–2.43 (m, 2H, H4), 2.31–2.20 (m, 6H, H5/H14/H23), 1.96 (s, 3H, H31), 1.82–1.74 (m, 2H, H1), 1.53–1.44 (m, 6H, H10/H19/H28), 1.41–1.32 (m, 6H, H8/H17/H26), 1.25–1.15 (m, 6H, H9/H18/H27) ppm. ^{13}C NMR (125.81 MHz, DMSO-d_6): δ 180.1 (C4′), 177.0 (C2′/C3′), 172.4 (C7′/C9′), 171.9–171.8 (C5′/C8′/C10′), 170.6 (C11′), 56.1 (C1′), 47.6–47.3 (C11/C20/C29), 38.9 (C7/C16/C25), 32.7 (C4), 32.0 (C5), 31.4 (C2/C3), 30.3 (C14/C23), 29.3 (C8/C17/C26), 28.0 (C13/C22), 26.5 (C10/C19/C28), 24.0 (C9/C18/C27), 20.8 (C31), 16.4 (C1) ppm. ^{15}N NMR (50.70 MHz, DMSO-d_6): δ −51.6 (NH_3), 94.9 (*N*H) ppm. ^{195}Pt NMR (107.55 MHz, DMSO-d_6): δ 3382 ppm. ESI-HRMS$^+$ found (calculated): m/z $[M + Na^+]^+$, 1070.3984 (1070.3983); $[M + H^+]^+$, 1048.4165 (1048.4163); $[M + 2Na^+]^{2+}$, 546.6940 (546.6917). ESI-HRMS$^-$ found (calculated): m/z $[M - H^+]^-$, 1046.4016 (1046.4018); $[M - 2H^+]^{2-}$, 522.6983 (522.6941). Analytical UHPLC (mobile phase: water/MeOH, 65/45): t_R = 1.09 min (84%), 0.95 (~12%). Elemental analysis, found: C, 39.81; H, 5.98; N, 10.74. Calc. for $C_{35}H_{64}N_8O_{16}Pt{\cdot}0.5\ H_2O$: C, 39.77; H, 6.20; N, 10.60%.

(*OC*-6-44)-(Acetato)diammine(cyclobutane-1,1-dicarboxylato)(3,14,25-trihydroxy-2,10,13,21,24,32-hexaoxo-3,9,14,20,25,31-hexaazapentatriacontan-35-oato)platinum(IV) (B). **3** (448 mg, 0.82 mmol) and CDI (146 mg, 0.90 mmol) in DMF (19 mL); DFO·mes (538 mg, 0.82 mmol) and TEA (228 μL, 1.64 mmol) in DMSO (6 mL). Preparative RP-HPLC gradient conditions

(H_2O/MeOH): 0–6 min (21% MeOH), 6–18.0 min (21–60% MeOH), 18.1–23.0 min (95% MeOH), 23.1–25.0 min (21% MeOH); the product eluted at 18.0 min. Yield (187 mg, 21%). ^{1}H NMR (500.32 MHz, DMSO-d_6): δ 9.68 (s, 1H, H30), 9.63 (s, 2H, H12/H21), 7.81 (s, 3H, H6″/H15/H24), 6.57–6.12 (m, 6H, NH_3), 3.50–3.42 (m, 6H, H11/H20/H29), 3.05–2.95 (d, J 5.4 Hz, 6H, H7/H16/H25), 2.62–2.55 (m, 4H, H13/H22), 2.50 (under DMSO, 4H, H2/H3), 2.46–2.42 (m, 2H, H4), 2.26 (dt, J 14.8 Hz, 6H, H5/H14/H23), 1.97 (s, 3H, H6), 1.90 (s, 3H, H31), 1.86–1.77 (m, 2H, H1), 1.55–1.45 (m, 6H, H8/H17/H26), 1.42–1.33 (m, 6H, H10/H19/H28), 1.26–1.16 (m, 6H, H9/H18/H27) ppm. ^{13}C NMR (125.81 MHz, DMSO-d_6): δ 179.6 (C4′), 177.7 (C6′), 176.7 (C2′/C3′), 172.4 (C5′), 171.7–171.5 (C7′/C8′/C9′/C10′), 170.6 (C11′), 56.0 (C1′), 47.5 (C11/C20), 47.2 (C29), 38.9 (C7/C16/C25), 32.0 (C13/C22), 31.6 (C14/C23), 31.3 (C4), 30.3 (C-5), 29.3 (C8/C17/C26), 28.0 (C2/C3), 26.5 (C9/C18/C27), 24.0 (C10/C19/C28), 23.0 (C6), 20.8 (C31), 16.2 (C1) ppm. ^{15}N NMR (50.70 MHz, DMSO-d_6): δ −53.0 (NH_3), 95.0 (NH) ppm. ^{195}Pt NMR (107.55 MHz, DMSO-d_6): δ 3573 ppm. ESI-HRMS$^+$ found (calculated): m/z [M + Na^+]$^+$, 1112.4093 (1112.4089); [M + $2Na^+$]$^{2+}$, 567.6995 (567.6990). ESI-HRMS$^-$ found (calculated): m/z [M + Cl^-]$^-$, 1124.3904 (1124.3890); [M − H^+]$^-$, 1088.4136 (1088.4124). Analytical UHPLC (mobile phase: water/MeOH, 65/45): t_R = 1.33 min, purity > 98%. Elemental analysis, found: C, 39.50; H, 6.25; N, 9.80. Calc. for $C_{37}H_{66}N_8O_{17}Pt{\cdot}1.5\ H_2O$: C, 39.78; H, 6.23; N, 10.03%.

(*OC*-6-44)-Diammine(cyclobutane-1,1-dicarboxylato)(propionato)(3,14,25-trihydroxy-2,10,13,21,24,32-hexaoxo-3,9,14,20,25,31-hexaazapentatriacontan-35-oato)platinum(IV) (C). 4 (403 mg, 0.72 mmol) and CDI (134 mg, 0.83 mmol) in DMF (10 mL); DFO·mes (492 mg, 0.75 mmol) and TEA (208 μL, 1.50 mmol) in DMSO (6 mL). Preparative RP-HPLC gradient conditions (H_2O/MeOH): 0.0–6.0 min (50% MeOH), 6.0–13.5 min (50–75% MeOH), 13.6–18.7 min (95% MeOH), 18.8–20.7 min (50% MeOH); the product eluted at 8.9 min. Yield (83 mg, 10%). ^{1}H NMR (500.32 MHz, DMSO-d_6): δ 9.69 (s, 1H, H30), 9.64 (s, 2H, H12/H21), 7.84–7.76 (m, 3H, H6″/H15/H24), 6.53–6.16 (m, 6H, NH_3), 3.50–3.43 (m, 6H, H11/H20/H29), 3.04–2.96 (m, 6H, H7/H16/H25), 2.61–2.55 (m, 4H, H13/H22), 2.50 (under DMSO, 6H, H2/H3/H6), 2.45–2.41 (m, 2H, H4), 2.31–2.20 (m, 6H, H5/H14/H23), 1.90 (s, 3H, H31), 1.86–1.76 (m, 2H, H1), 1.54–1.45 (m, 6H, H8/H17/H26), 1.43–1.32 (m, 6H, H10/H19/H28), 1.27–1.16 (m, 6H, H9/H18/H27), 0.93 (t, J 7.5 Hz, 3H, H32) ppm. ^{13}C NMR (125.81 MHz, DMSO-d_6): δ 180.4 (C6′), 179.7 (C4′), 176.8 (C2′/C3′), 172.4 (C5′), 171.8–171.7 (C7′/C8′/C9′/C10′), 170.6 (C11′), 56.0 (C1′), 47.5 (C11/C20), 47.2 (C29), 38.9 (C7/C16/C25), 32.0 (C13/C22), 31.6 (C14/C23), 31.4 (C4), 30.3 (C5), 29.3 (C8/C17/C26), 28.8 (C2), 28.0 (C3), 26.5 (C9/C18/C27), 24.0 (C10/C19/C28), 23.0 (C6), 20.8 (C31), 16.2 (C1), 10.4 (C32) ppm. ^{15}N NMR (50.70 MHz, DMSO-d_6): δ −51.8 (NH_3), 95.3 (NH) ppm. ^{195}Pt NMR (107.55 MHz, DMSO-d_6): δ 3574 ppm. ESI-HRMS$^+$ found (calculated): m/z [M + Na^+]$^+$, 1126.4219 (1126.4245); [M + $2Na^+$]$^{2+}$, 574.7057 (574.7069). ESI-HRMS$^-$ found (calculated): m/z [M − H^+]$^-$, 1102.4295 (1102.4269); [M − $2H^+$]$^{2-}$, 550.7119 (550.7093). Analytical UHPLC (mobile phase: water/MeOH, 65/45): t_R = 1.91 min, purity > 99%. Elemental analysis, found: C, 40.18; H, 6.22; N, 9.76. Calc. for $C_{38}H_{68}N_8O_{17}Pt{\cdot}1.5\ H_2O$: C, 40.35; H, 6.33; N, 9.91%.

(*OC*-6-44)-Diammine(3-carboxypropanoato)(cyclobutane-1,1-dicarboxylato) (3,14,25-trihydroxy-2,10,13,21,24,32-hexaoxo-3,9,14,20,25,31-hexaazapentatriacontan-35-oato)platinum(IV) (D) and (*OC*-6-33)-diammine(cyclobutane-1,1-dicarboxylato) bis(3,14,25-trihydroxy-2,10,13,21,24,32-hexaoxo-3,9,14,20,25,31-hexaazapentatriacontan-35-oato)platinum(IV) (E). 5 (199 mg, 0.33 mmol) and CDI (112 mg, 0.69 mmol) in DMF (10 mL); DFO·mes (432 mg, 0.66 mmol) and TEA (190 μL, 1.36 mmol) in DMSO (6 mL). Preparative RP-HPLC gradient conditions (H_2O/MeCN): 0.0–6.0 min (10% MeCN), 6.0–21.0 min (10–35% MeCN), 21.1–26.0 min (95% MeCN), 26.1–28.1 min (10% MeCN); the products eluted at 17.1 min (**D**) and 18.8 min (**E**). Yield: **D** (51 mg, 18%), **E** (24 mg, 10%).

*Characterization **D**.* ^{1}H NMR (500.32 MHz, DMSO-d_6): δ 9.66 (s, 4H, H12/H21/H30/H32), 7.81 (s, 3H, H6/H15/H24), 6.51–6.17 (m, 6H, NH_3), 3.49–3.42 (m, 6H, H11/H20/H29), 3.03–2.96 (m, 6H, H7/H16/H25), 2.61–2.54 (m, 4H, H13/H22), 2.50 (under DMSO, 4H, H2/H3), 2.47–2.43 (m, 2H, H4), 2.37–2.31 (m, 2H, H4″), 2.30–2.21 (m, 6H, H5/H14/H23), 1.97 (s, 3H, H31), 1.85–1.77 (m, 2H, H1), 1.54–1.45 (m, 6H, H8/H17/H26), 1.42–1.34 (m, 6H, H10/H19/H28), 1.26–1.17 (m, 6H, H9/H18/H27) ppm. ^{13}C NMR (125.81 MHz, DMSO-d_6): δ 180.1 (C6′), 179.6 (C4′), 176.8 (C2′/C3′), 174.3 (C5″), 172.4 (C5′), 171.8–171.6 (C7′/C8′/C9′/C10′), 171.5 (C11′), 56.0 (C1′), 47.5 (C11/C20), 47.2 (C29), 38.9 (C7/C16/C25), 31.7 (C13/C22), 31.6 (C14/C23), 31.3 (C4), 30.6 (5″), 30.3 (C5), 29.2 (C8/C17/C26), 28.0 (C2/C3), 26.5 (C9/C18/C27), 24.0 (C10/C19/C28), 20.8 (C31), 16.2 (C1) ppm. ^{15}N NMR (50.70 MHz, DMSO-d_6): δ −52.7 (NH_3), 94.7 (NH_2) ppm. ^{195}Pt NMR (107.55 MHz, DMSO-d_6): δ 3580 ppm. ESI-HRMS$^+$ found (calculated): m/z [M + Na^+]$^+$, 1170.4133 (1170.4144); [M + $2Na^+$]$^{2+}$, 596.7015 (596.7018). ESI-HRMS$^-$ found (calculated): m/z [M − H^+]$^-$, 1146.4190 (1146.4179); [M − $2H^+$]$^-$, 572.7073 (572.7053). Analytical UHPLC (mobile phase: water/MeOH, 65/45): t_R = 1.31 min, purity > 98%. Elemental analysis, found: C, 39.93; H, 6.08; N, 9.44. Calc. for $C_{39}H_{68}N_8O_{19}Pt{\cdot}1.0\ H_2O$: C, 40.17; H, 6.05; N, 9.61%.

*Characterization **E**.* ^{1}H NMR (500.32 MHz, DMSO-d_6): δ 9.68 (s, 6H, H12/H21/H30), 7.81 (s, 6H, H6/H15/H24), 6.53–6.16 (m, 6H, NH_3), 3.49–3.41 (m, 12H, H11/H20/H29), 3.04–2.96 (m, 12H, H7/H16/H25), 2.61–2.55 (m, 8H, H13/H22), 2.50 (under DMSO, 4H, H2/H3), 2.47–2.42 (m, 4H, H4), 2.30–2.20 (m, 12H, H5/H14/H23), 1.97 (s, 6H, H31), 1.85–1.77 (m, 2H, H1), 1.54–1.44 (m, 12H, H8/H17/H26), 1.42–1.33 (m, 12H, H10/H19/H28), 1.27–1.16 (m, 12H, H9/H18/H27) ppm. ^{13}C NMR (125.81 MHz, DMSO-d_6): δ 179.5 (C4′), 176.8 (C2′/C3′), 172.4 (C5′), 171.8–171.5 (C7′/C8′/C9′/C10′), 170.6 (C11′), 56.0 (C1′), 47.5 (C11/C20), 47.2 (C29), 38.9 (C7/C16/C25), 31.7 (C13/C22), 31.6 (C14/C23), 31.3 (C4), 30.3 (C5), 29.2 (C8/C17/C26), 28.0 (C2/C3), 26.5 (C9/C18/C27), 24.0 (C10/C19/C28), 20.8 (C31), 16.2 (C1) ppm. ^{15}N NMR (50.70 MHz, DMSO-d_6): δ −52.7 (NH_3), 94.8 (NH) ppm. ^{195}Pt NMR (107.55 MHz, DMSO-d_6): δ 3576 ppm. ESI-HRMS$^+$ found (calculated): m/z [M + Na^+]$^+$,

1712.7592 (1712.7572); $[M + 2Na^+]^{2+}$, 867.8735 (867.8732); $[M + 3Na^+]^{3+}$, 586.2452 (586.2452). ESI-HRMS$^-$ found (calculated): m/z $[M - H^+]^-$, 1688.7665 (1688.7607); $[M - 2H^+]^{2-}$, 843.8815 (843.8767); $[M - 3H^+]^{3-}$, 562.2525 (562.2487). Analytical UHPLC (mobile phase: water/MeOH, 65/45): t_R = 4.71 min, purity > 96%. Elemental analysis, found: C, 43.96; H, 6.78; N, 11.02. Calc. for $C_{64}H_{114}N_{14}O_{26}Pt{\cdot}2.5\ H_2O$: C, 44.28; H, 6.91; N, 11.30%.

Lipophilicity determination

Chromatographic lipophilicity parameters were assessed by means of RP-HPLC as described previously.[49,62] Chromatograms for each compound were run in duplicates in isocratic mode with at least three different water/methanol mobile phase compositions. KI was used as an external reference to determine the column dead time (t_0). Capacity factors, $k = (t_R - t_0)/t_0$, were calculated for all the investigated eluent compositions and used to derive lipophilicity parameters $\log k_w$ and φ_0. $\log k_w$ is defined as the logarithmic capacity factor of a compound in a mobile phase containing pure water, while φ_0 corresponds to the volume percentage of the organic modifier in the mobile phase at which the analyte is equally distributed in the mobile and the stationary phase.[49]

Stability studies

Pt(IV)–DFO complexes (c = 0.5 mM) were incubated in water and PBS (pH 7.4) at ambient temperature for 24 h. RP-UHPLC measurements were conducted immediately after dissolving and after 1, 5 and 24 h to monitor stability of the compounds. Gradient eluent conditions with MeCN/water (*e.g.*, 5–85% MeCN in 6 min, 85–95% MeCN in 2 min) were used.

Reactivity of complexes **B** and **D** towards ascorbic acid was monitored by ^{1}H NMR spectroscopy at 25 °C in 50 mM phosphate buffer (in D_2O, pD 7.4). The complexes were dissolved in the buffer solution and their stability at this experimental setting was verified by measuring ^{1}H NMR spectra from time to time over a period of 24 h. Subsequently, ascorbic acid was added to the samples to yield final concentrations of 1 mM complex and 25 mM ascorbic acid, and ^{1}H NMR spectra were recorded for 1 week.

Incubation with metal salts

Stock solutions of $FeCl_3$, $ZnCl_2$, $ZrCl_4$ and Pt(IV)–DFO complexes under investigation were prepared in Milli-Q water (with addition of 1% DMSO for solubilization, when needed). Subsequently, mixtures containing complex and the respective metal salt in ratios of 2 : 1, 1 : 1 and 1 : 2 (complex concentration of 0.5 mM) were prepared and incubated for 24 h at 25 °C. Complexation reactions were followed by RP-UHPLC, employing gradient eluent conditions with MeCN/water; UV-visible detection was set at 210, 225 and 450 nm. Adducts formation was further examined by ESI-HRMS.

Iron(III) binding of compounds B, D and DFO, and cyclic voltammetry

UV-visible spectra were recorded for the Fe(III) complex **B** or **D** or DFO (1 : 1) systems on an Agilent Cary 8454 diode array spectrophotometer at pH 0.71–11.5, and at pH 7.4 (50 mM HEPES) in the presence of deferiprone (Sigma-Aldrich, up to 72.2 excess) at 25 °C and 0.20 M KCl ionic strength. The path length was 1 cm. Conditional stability constants of the complexes were calculated with the computer program PSEQUAD.[63]

Cyclic voltammograms of the Fe(III) complexes of compound **B** or **D** were measured at 25.0 ± 0.1 °C and at an ionic strength of 0.2 M (KNO_3) on samples containing 0.5 mM $FeCl_3$ and 0.5 mM Pt(IV) complex at pH 7.4 in aqueous solution. The pH of the samples was adjusted by the addition of minor amount of HNO_3 and KOH solutions. Samples were purged for 15 min with argon before recording the voltammograms. Measurements were performed on a conventional three-electrode system under argon atmosphere and a PC controlled Autolab-PGSTAT 204 potentiostat at a scan rate of 10 mV s^{-1}. Platinum working and auxiliary electrodes and a Ag/AgCl/KCl (3 M) reference electrode were used. Potentials are given as relative to NHE. The electrochemical measuring system was calibrated with $K_3[Fe(CN)_6]$.

Cell lines and culture conditions

CH1/PA-1 ovarian teratocarcinoma cells were kindly provided by Lloyd R. Kelland (CRC Centre for Cancer Therapeutics, Institute of Cancer Research, Sutton, UK), and SW480 colon carcinoma as well as A549 non-small cell lung cancer cells by the Institute of Cancer Research, Department of Medicine I, Medical University of Vienna, Austria. Cells were maintained in minimal essential medium (MEM), supplemented with 10% v/v heat-inactivated fetal calf serum (FCS; from BioWest), 4 mM L-glutamine, 1 mM sodium pyruvate and 1% v/v non-essential amino acid solution, as adherent monolayer cultures in 75 cm^2 flasks, from which they were harvested by trypsinization. All cell culture media, supplements and reagents were purchased from Sigma-Aldrich and all plasticware from Starlab, unless stated otherwise. All incubations were at 37 °C under a humidified atmosphere containing 5% CO_2 in air.

Cytotoxicity assays

For tests in monolayer cultures, 1 × 10^3 CH1/PA-1, 2 × 10^3 SW480 or 3 × 10^3 A549 cells per well were seeded in 100 µl per well aliquots of supplemented MEM into flat-bottom 96-well microculture plates. After 24 h incubation, stock solutions of the test compounds were prepared in supplemented MEM, except for compound **E** which required dissolution in DMSO (Fisher Scientific), and serially diluted in the same medium. For combinations of **B** with $FeCl_3$ (molar ratio of 1 : 1) as well as carboplatin with DFO (molar ratios of 1 : 1 and 1 : 2), appropriately concentrated solutions were mixed and mixtures serially diluted prior to their application. 100 µl per well aliquots of each dilution were added to the plates in triplicates (with

final DMSO content not exceeding 0.5% v/v for **E**). After incubation for 96 h, MEM was exchanged for 100 μl per well of a 1 : 7 v/v mixture of MTT dye (5 mg mL^{-1} 3-(4,5-dimethylthiazol-2-yl)-2,5-diphenyl-2*H*-tetrazolium bromide in phosphate-buffered saline) and RPMI 1640 medium (supplemented with 10% FCS and 4 mM L-glutamine). After incubation for another 4 h, mixtures were replaced with 150 μl DMSO per well and optical densities were measured with a microplate reader (BioTek ELx808) at 550 nm (and 690 nm as a reference).

For tests in multicellular tumor spheroids, the fluorimetric resazurin assay was employed. For this purpose, 1×10^3 CH1/PA-1 cells per well were seeded in 100 μl per well aliquots of supplemented MEM into round-bottom ultra-low attachment 96-well plates (Nunclon Sphera™). After four days of spheroid formation and growth, test compounds were applied as described above. For the last 20 h of another 96 h incubation period, 20 μL per well of a 440 μM solution of resazurin sodium salt in phosphate-buffered saline were added without prior dissociation of the spheroids, and thereafter fluorescence (excitation 530 nm/emission 590 nm) was measured with a Synergy HT reader (BioTek).

All results are averages from at least three independent experiments, and 50% inhibitory concentrations (IC_{50}) relative to untreated controls were interpolated from concentration-effect curves.

Combination effects between carboplatin and DFO were further assessed by using the median-effect principle – combination index (MEP-CI) method of Chou and Talalay.[59] The interactions between the drugs were computed in terms of CI over the entire range of cell viability (from 3% to 95%) with CompuSyn software.[60] CI = 1 indicates an additive effect, CI < 1 synergism and CI > 1 antagonism. Sequential deletion analysis (S.D.A.) was used as a measure of the variability of the CI values at presented effect levels. Means ± 95% confidence intervals were calculated at the specified effect levels after an iterative sequential deletion of one concentration of a drug at a time for repetitive CI calculations.[59,60]

Conflicts of interest

There are no conflicts to declare.

Acknowledgements

The support of the Austrian Science Fund (FWF, Project number: J3577-B13) and the Ministry of Human Capacities of Hungary (Grant TKP-2020) is gratefully acknowledged.

References

1 B. Rosenberg, L. Van Camp, J. E. Trosko and V. H. Mansour, *Nature*, 1969, **222**, 385–386.
2 S. Dasari and P. B. Tchounwou, *Eur. J. Pharmacol.*, 2014, **740**, 364–378.
3 L. Kelland, *Nat. Rev. Cancer*, 2007, **7**, 573–584.
4 D. M. Cheff and M. D. Hall, *J. Med. Chem.*, 2017, **60**, 4517–4532.
5 R. Oun, Y. E. Moussa and N. J. Wheate, *Dalton Trans.*, 2018, **47**, 6645–6653.
6 V. J. Stella, *Expert Opin. Ther. Pat.*, 2004, **14**, 277–280.
7 E. R. Jamieson and S. J. Lippard, *Chem. Rev.*, 1999, **99**, 2467–2498.
8 T. C. Johnstone, K. Suntharalingam and S. J. Lippard, *Chem. Rev.*, 2016, **116**, 3436–3486.
9 S. Theiner, H. P. Varbanov, M. Galanski, A. E. Egger, W. Berger, P. Heffeter and B. K. Keppler, *J. Biol. Inorg. Chem.*, 2015, **20**, 89–99.
10 M. D. Hall, H. R. Mellor, R. Callaghan and T. W. Hambley, *J. Med. Chem.*, 2007, **50**, 3403–3411.
11 U. Basu, B. Banik, R. Wen, R. K. Pathak and S. Dhar, *Dalton Trans.*, 2016, **45**, 12992–13004.
12 M. R. Reithofer, A. K. Bytzek, S. M. Valiahdi, C. R. Kowol, M. Groessl, C. G. Hartinger, M. A. Jakupec, M. Galanski and B. K. Keppler, *J. Inorg. Biochem.*, 2011, **105**, 46–51.
13 I. F. Tannock and D. Rotin, *Perspect. Cancer Res.*, 1989, **49**, 4373–4384.
14 D. Gibson, *Dalton Trans.*, 2016, **45**, 12983–12991.
15 R. J. Schilder, F. P. LaCreta, R. P. Perez, S. W. Johnson, J. M. Brennan, A. Rogatko, S. Nash, C. McAleer, T. C. Hamilton, D. Roby, R. C. Young, R. F. Ozols and P. J. O'Dwyer, *Cancer Res.*, 1994, **54**, 709–717.
16 C. Trask, A. Silverstone, C. M. Ash, H. Earl, C. Irwin, A. Bakker, J. S. Tobias and R. L. Souhami, *J. Clin. Oncol.*, 1991, **9**, 1131–1137.
17 N. J. Wheate, S. Walker, G. E. Craig and R. Oun, *Dalton Trans.*, 2010, **39**, 8113.
18 H. Song, H. Xiao, Y. Zhang, H. Cai, R. Wang, Y. Zheng, Y. Huang, Y. Li, Z. Xie, T. Liu and X. Jing, *J. Mater. Chem. B*, 2013, **1**, 762–772.
19 D. Gibson, *J. Inorg. Biochem.*, 2019, **191**, 77–84.
20 E. Gabano, M. Ravera and D. Osella, *Dalton Trans.*, 2014, **43**, 9813.
21 S. Dhar and S. J. Lippard, *Proc. Natl. Acad. Sci. U. S. A.*, 2009, **106**, 22199–22204.
22 W. H. Ang, I. Khalaila, C. S. Allardyce, L. Juillerat-Jeanneret and P. J. Dyson, *J. Am. Chem. Soc.*, 2005, **127**, 1382–1383.
23 K. G. Z. Lee, M. V. Babak, A. Weiss, P. J. Dyson, P. Nowak-Sliwinska, D. Montagner and W. H. Ang, *ChemMedChem*, 2018, **13**, 1210–1217.
24 W. Neumann, B. C. Crews, M. B. Sárosi, C. M. Daniel, K. Ghebreselasie, M. S. Scholz, L. J. Marnett and E. Hey-Hawkins, *ChemMedChem*, 2015, **10**, 183–192.
25 Q. Cheng, H. Shi, H. Wang, Y. Min, J. Wang and Y. Liu, *Chem. Commun.*, 2014, **50**, 7427–7430.
26 J. Yang, X. Sun, W. Mao, M. Sui, J. Tang and Y. Shen, *Mol. Pharm.*, 2012, **9**, 2793–2800.
27 R. Raveendran, J. P. Braude, E. Wexselblatt, V. Novohradsky, O. Stuchlikova, V. Brabec, V. Gandin and D. Gibson, *Chem. Sci.*, 2016, **7**, 2381–2391.

28 L. Ma, R. Ma, Y. Wang, X. Zhu, J. Zhang, H. C. Chan, X. Chen, W. Zhang, S. K. Chiu and G. Zhu, *Chem. Commun.*, 2015, **51**, 6301–6304.
29 E. Petruzzella, R. Sirota, I. Solazzo, V. Gandin and D. Gibson, *Chem. Sci.*, 2018, **9**, 4299–4307.
30 W. Hu, L. Fang, W. Hua and S. Gou, *J. Inorg. Biochem.*, 2017, **175**, 47–57.
31 M. V. Babak, Y. Zhi, B. Czarny, T. B. Toh, L. Hooi, E. K. Chow, W. H. Ang, D. Gibson and G. Pastorin, *Angew. Chem., Int. Ed.*, 2019, **58**, 8109–8114.
32 E. Petruzzella, J. P. Braude, J. R. Aldrich-Wright, V. Gandin and D. Gibson, *Angew. Chem., Int. Ed.*, 2017, **56**, 11539–11544.
33 N. F. Olivieri and G. M. Brittenham, *Blood*, 1997, **89**, 739–761.
34 S. Abbina, U. Abbasi, A. Gill, K. Wong, M. T. Kalathottukaren and J. N. Kizhakkedathu, *ACS Cent. Sci.*, 2019, 917–926.
35 G. Fischer, U. Seibold, R. Schirrmacher, B. Wängler and C. Wängler, *Molecules*, 2013, **18**, 6469–6490.
36 M. P. Gotsbacher, T. J. Telfer, P. K. Witting, K. L. Double, D. I. Finkelstein and R. Codd, *Metallomics*, 2017, **9**, 852–864.
37 Z. Estrov, A. Cohen, E. W. Gelfand and M. H. Freedman, *Toxicol. Vitr.*, 1988, **2**, 131–134.
38 Y. S. Lee and R. D. Wurster, *Toxicol. Lett.*, 1995, **78**, 67–71.
39 T. Yamasaki, S. Terai and I. Sakaida, *N. Engl. J. Med.*, 2011, **365**, 576–578.
40 Y. Yu, Z. Kovacevic and D. R. Richardson, *Cell Cycle*, 2007, **6**, 1982–1994.
41 H. P. Varbanov, F. Kuttler, D. Banfi, G. Turcatti and P. J. Dyson, *PLoS One*, 2019, **14**, e0211268.
42 D. Höfer, H. P. Varbanov, A. Legin, M. A. Jakupec, A. Roller, M. Galanski and B. K. Keppler, *J. Inorg. Biochem.*, 2015, **153**, 259–271.
43 A. R. Z. Almotairy, V. Gandin, L. Morrison, C. Marzano, D. Montagner and A. Erxleben, *J. Inorg. Biochem.*, 2017, **177**, 1–7.
44 H. P. Varbanov, S. M. Valiahdi, C. R. Kowol, M. A. Jakupec, M. Galanski and B. K. Keppler, *Dalton Trans.*, 2012, **41**, 14404–14415.
45 M. Reithofer, M. Galanski, A. Roller and B. K. Keppler, *Eur. J. Inorg. Chem.*, 2006, **2006**, 2612–2617.
46 H. P. Varbanov, S. Göschl, P. Heffeter, S. Theiner, A. Roller, F. Jensen, M. A. Jakupec, W. Berger, M. Galanski and B. K. Keppler, *J. Med. Chem.*, 2014, **57**, 6751–6764.
47 S. Göschl, H. P. Varbanov, S. Theiner, M. A. Jakupec, M. Galanski and B. K. Keppler, *J. Inorg. Biochem.*, 2016, **160**, 264–274.
48 L. Ayouni, G. Cazorla, D. Chaillou, B. Herbreteau, S. Rudaz, P. Lantéri and P.-A. Carrupt, *Chromatographia*, 2005, **62**, 251–255.
49 M. Klose, S. Theiner, H. Varbanov, D. Hoefer, V. Pichler, M. Galanski, S. Meier-Menches and B. Keppler, *Inorganics*, 2018, **6**, 130.
50 E. Farkas, É. A. Enyedy and H. Csóka, *Polyhedron*, 1999, **18**, 2391–2398.
51 H. Keberle, *Ann. N. Y. Acad. Sci.*, 1964, **119**, 758–768.
52 Y. Bentur, M. McGuigan and G. Koren, *Drug Saf.*, 1991, **6**, 37–46.
53 A. Evers, R. D. Hancock, A. E. Martell and R. J. Motekaitis, *Inorg. Chem.*, 1989, **28**, 2189–2195.
54 I. Spasojević, S. K. Armstrong, T. J. Brickman and A. L. Crumbliss, *Inorg. Chem.*, 1999, **38**, 449–454.
55 E. Farkas, H. Csóka, G. Micera and A. Dessi, *J. Inorg. Biochem.*, 1997, **65**, 281–286.
56 E. T. Clarke and A. E. Martell, *Inorg. Chim. Acta*, 1992, **196**, 185–194.
57 A. S. Nunes, A. S. Barros, E. C. Costa, A. F. Moreira and I. J. Correia, *Biotechnol. Bioeng.*, 2019, **116**, 206–226.
58 E. Schreiber-Brynzak, E. Klapproth, C. Unger, I. Lichtscheidl-Schultz, S. Göschl, S. Schweighofer, R. Trondl, H. Dolznig, M. A. Jakupec and B. K. Keppler, *Invest. New Drugs*, 2015, **33**, 835–847.
59 T.-C. Chou, *Pharmacol. Rev.*, 2006, **58**, 621–681.
60 T.-C. Chou and N. Martin, *CompuSyn for Drug Combinations: PC Software and User's Guide*, ComboSyn, Inc., Paramus, (NJ), 2005, http://www.combosyn.com.
61 F. D. Rochon and L. M. Gruia, *Inorg. Chim. Acta*, 2000, **306**, 193–204.
62 D. Höfer, H. P. Varbanov, M. Hejl, M. A. Jakupec, A. Roller, M. Galanski and B. K. Keppler, *J. Inorg. Biochem.*, 2017, **174**, 119–129.
63 L. Zékány and I. Nagypál, *Computational Methods for the Determination of Stability Constants*, ed. D. L. Leggett, Plenum Press, New York, 1985.